Archives of Microbiology (2024) 206:321
https://doi.org/10.1007/s00203-024-04060-x

ORIGINAL PAPER

IcmF2 of the type VI secretion system 2 plays a role in biofilm formation of *Vibrio parahaemolyticus*

Qinglian Huang[1,2] · Miaomiao Zhang[2] · Yiquan Zhang[2] · Xue Li[2] · Xi Luo[2] · Shenjie Ji[1] · Renfei Lu[2]

Received: 9 May 2024 / Revised: 17 June 2024 / Accepted: 18 June 2024 / Published online: 22 June 2024

Abstract

Vibrio parahaemolyticus possesses two distinct type VI secretion systems (T6SS), namely T6SS1 and T6SS2. T6SS1 is predominantly responsible for adhesion to Caco-2 and HeLa cells and for the antibacterial activity of *V. parahaemolyticus*, while T6SS2 mainly contributes to HeLa cell adhesion. However, it remains unclear whether the T6SS systems have other physiological roles in *V. parahaemolyticus*. In this study, we demonstrated that the deletion of *icmF2*, a structural gene of T6SS2, reduced the biofilm formation capacity of *V. parahaemolyticus* under low salt conditions, which was also influenced by the incubation time. Nonetheless, the deletion of *icmF2* did not affect the biofilm formation capacity in marine-like growth conditions, nor did it impact the flagella-driven swimming and swarming motility of *V. parahaemolyticus*. IcmF2 was found to promote the production of the main components of the biofilm matrix, including extracellular DNA (eDNA) and extracellular proteins, and cyclic di-GMP (c-di-GMP) in *V. parahaemolyticus*. Additionally, IcmF2 positively influenced the transcription of *cpsA*, *mfpA*, and several genes involved in c-di-GMP metabolism, including *scrJ*, *scrL*, *vopY*, *tpdA*, *gefA*, and *scrG*. Conversely, the transcription of *scrA* was negatively impacted by IcmF2. Therefore, IcmF2-dependent biofilm formation was mediated through its effects on the production of eDNA, extracellular proteins, and c-di-GMP, as well as its impact on the transcription of *cpsA*, *mfpA*, and genes associated with c-di-GMP metabolism. This study confirmed new physiological roles for IcmF2 in promoting biofilm formation and c-di-GMP production in *V. parahaemolyticus*.

Keywords Vibrio parahaemolyticus · T6SS2 · IcmF2 · Biofilm formation · c-di-GMP · Regulation

Introduction

The type VI secretion system (T6SS) is a widespread, bacteriophage-like complex in Gram-negative bacteria that delivers effector proteins into target cells in a contact-dependent manner (Hespanhol et al. 2023). The system was initially described as a virulence factor of *Pseudomonas aeruginosa* in cystic fibrosis (CF) patients because Hcp1, secreted by T6SS, and its specific antibodies were detected in these patients (Mougous et al. 2006). It was found that *hcp* genes are consistently embedded within the T6SS gene cluster and are adjacent to *vgrG* genes, which encode a crucial structural protein of the T6SS (Mougous et al. 2006; Pukatzki et al. 2006; Ma et al. 2012). In *Vibrio cholerae*, deletion of *hcp* blocks the secretion of VgrG, and the deletion of *vgrG* similarly affects the secretion of Hcp (Pukatzki et al. 2006). Hcp proteins are required for the mature biofilm formation of *P. aeruginosa*, but they do not reduce biofilm formation (Gallique et al. 2017b). T6SS also functions as a cell-to-cell

Qinglian Huang and Miaomiao Zhang contributed equally to this work.

Communicated by Yusuf Akhter.

✉ Yiquan Zhang
zhangyiquanq@163.com

✉ Shenjie Ji
1275558317@qq.com

✉ Renfei Lu
rainman78@163.com

[1] Department of Clinical Laboratory, Qidong People's Hospital, Qidong, Jiangsu 226200, China

[2] Department of Clinical Laboratory, Nantong Third People's Hospital, Affiliated Nantong Hospital 3 of Nantong University, Nantong, Jiangsu 226006, China

signal that promotes interbacterial communication depending on cell density (Gallique et al. 2017a). Furthermore, T6SS is utilized as an antibacterial weapon to kill rival bacteria in polymicrobial environments (Coulthurst 2013). T6SS-dependent bacterial killing against rival bacteria is considered a mechanism for pathogens to successfully colonize the host gut (Sana et al. 2016). Additionally, T6SS is also required for metal ion uptake and resistance to stress and host immunity (Wang et al. 2015). In summary, T6SS contributes to multiple bacterial behaviors, including colonization, pathogenesis, interbacterial interactions, biofilm formation, stress resistance, and ion uptake.

V. parahaemolyticus is a leading cause of seafood-associated gastroenteritis and can form stable biofilms on surfaces, which are surface-associated bacterial communities that serves as a strategy for bacteria to resist unfavorable environments (Sharan et al. 2022). The biofilm matrix, which forms a living environment for the cells, is mainly composed of exopolysaccharides (EPS), proteins, extracellular DNA (eDNA), and lipids (Flemming and Wingender 2010). The levels of proteins and eDNA in the biofilm matrix are strongly and positively correlated with biofilm formation in *V. parahaemolyticus* (Li et al. 2020). EPS and the genes associated with their synthesis also influence colony morphology and biofilm formation of *V. parahaemolyticus* (Liu et al. 2022; Wu et al. 2022). Furthermore, biofilm formation is strictly regulated by various factors, including quorum sensing and cyclic di-GMP (c-di-GMP) (Lu et al. 2018; Park and Sauer 2022). Biofilms formed by *V. parahaemolyticus* pose a serious threat to public health and can cause significant economic losses in the food industry (Sharan et al. 2022).

V. parahaemolyticus possesses two distinct T6SS gene loci located on chromosomes 1 and 2, termed T6SS1 (VP1386-1420) and T6SS2 (VPA1024-1046), respectively (Makino et al. 2003). T6SS1 can be detected in clinical isolates and all environmental strains causing acute hepatopancreatic necrosis disease, and it predominantly contributes to cell adhesion and antibacterial activity of *V. parahaemolyticus* (Yu et al. 2012; Salomon et al. 2013; Li et al. 2017). By contrast, T6SS2 is found in all isolates from both environmental and clinical samples and mainly contributes to cell adhesion activity (Yu et al. 2012; Salomon et al. 2013). However, further research is needed to determine whether these two T6SSs have other physiological roles in *V. parahaemolyticus*, as studies have shown that T6SS functions are diverse in other bacterial species (Wang et al. 2015; Gallique et al. 2017a, b).

The T6SS2 gene cluster includes 22 genes organized into three putative operons: VPA1027-1025, VPA1043-1028, and VPA1044-1046 (Ma et al. 2012; Zhang et al. 2017). Among these, the *icmF2* gene (VPA1039) encodes the intracellular multiplication factor (IcmF), which acts as an inner-membrane protein of T6SS2 and is essential for the structure and function of T6SS2 in *V. parahaemolyticus* (Yu et al. 2012). Deletion of the *icmF2* gene reduces the adhesion activity of *V. parahaemolyticus* to HeLa monolayers (Yu et al. 2012). In this study, we investigated the role of the *icmF2* gene in biofilm formation of *V. parahaemolyticus*, using a combination of phenotypic and molecular approaches.

Materials and methods

Bacterial strains and growth conditions

V. parahaemolyticus RIMD2210633 was used as the wild type (WT) strain in this work. For construction of *icmF2* mutant (Δ*icmF2*), the entire coding region of *icmF2* was deleted from WT using the suicide plasmid pDS132, which was performed as previously described (Zhang et al. 2012). To complement the Δ*icmF2* strain (Sun et al. 2014), the coding region of *icmF2* was amplified using polymerase chain reaction (PCR) and then cloned into the pBAD33 vector. This vector contains an arabinose-induced P_{BAD} promoter and a chloramphenicol resistance gene. The recombinant plasmid was introduced into the Δ*icmF2* strain, yielding the complementation strain C-Δ*icmF2*. Control strains were created by transforming non-recombinant pBAD33 vector into both the WT and Δ*icmF2* strains, respectively.

For the cultivation of *V. parahaemolyticus* (Li et al. 2021), an overnight bacterial culture in Luria-Bertani (LB) broth containing 10 g/L tryptone (OXOID, UK), 5 g/L yeast extract (OXOID, UK), and 10 g/L NaCl (Solarbio, China; LB-1.0% NaCl) was diluted 50-fold into 5 ml of LB-1.0% NaCl and incubated at 37 °C until it reached to an OD_{600} value of 1.4, which served as the bacterial seed. The bacterial seed was further diluted 1000-fold into 5 ml of marine (M) broth (2.0% NaCl; BD Biosciences, USA), LB-0.5% NaCl, LB-1.0% NaCl, or LB-3.0% NaCl, in a 24-well cell culture plate (Corning Inc., Corning, USA). The plate was incubated at 30 °C with shaking at 150 rpm, and bacterial cells were harvested at specific time points. The final concentration of chloramphenicol was 5 µg/ml, and that of L-arabinose was 0.1% (w/v).

Crystal violet staining assay

Crystal violet (CV) staining assay was performed as previously described (Zhang et al. 2023d). Briefly, the bacterial seed was diluted 1,000-fold into 2 ml of M broth (or LB broth with different concentrations of NaCl) in a 24-well cell culture plate, and incubated at 30ºC with shaking at

150 rpm for specific durations. The OD_{600} value, indicative of planktonic cells in the medium, was measured using a spectrophotometer. The surface-attached cells were then washed with deionized water and stained with 0.1% CV. The bound CV was dissolved with 20% acetic acid, after which the OD_{570} was measured. Relative biofilm formation was expressed as the ratio OD_{570}/OD_{600}.

Colony morphology assay

The colony morphology assay was performed similarly to that previously described (Zhang et al. 2023d). Briefly, the bacterial seed was diluted 50-fold into 5 ml of M broth and then statically incubated at 30ºC for 24 h, followed by thorough mixing. Two microliters of the culture were spotted onto LB plates with varying concentrations of NaCl and then incubated statically at 30 °C for 48 h.

Measurement of growth curves

The bacterial seed was diluted 1, 000-fold into 10 ml of LB-0.5% NaCl, LB-1.0% NaCl, or LB-3.0% NaCl, mixed thoroughly, and then divided into a 96 well cell culture plate with 200 µl in each well. There were 8 replicates for each strain under each condition. Growth curves were created using a microbial growth curve analyzer MGC-200 (Ningbo Scientz Biotechnology Co. Ltd., China) at 37 °C, by detecting OD_{600} values at a 30 min interval (Li et al. 2024).

Motility assays

Motility assays were performed as previously described (Lu et al. 2019; Zhang et al. 2023c). Briefly, 2 µl of bacterial seed were inoculated into a semi-solid LB plate containing 0.5%, 1.0%, or 3.0% NaCl and 0.5% (w/v) Difco Noble agar (BD Biosciences, USA) for swimming motility. For warming motility, the seed was spotted onto a solid LB plate containing 0.5%, 1.0%, or 3.0% NaCl and 1.5% (w/v) Difco Noble agar. The diameters of swimming and swarming circles were measured after incubation at 37ºC for various durations.

Determination of eDNA and proteins in the biofilm matrix

The relative content of eDNA and proteins in the biofilm matrix were measured similarly to that previously described (Zhu et al. 2023). Briefly, equal amounts of surface-attached biofilms formed by the WT and Δ*icmF2* strains were washed twice with pre-cold phosphate-buffered solution (PBS), and then resuspended in 2 ml pre-cold 0.01 M KCl solution, followed by disruption with sonication. After centrifugation, the concentrations of total proteins and eDNA in the supernatant were measured using a Pierce BCA Protein Assay kit (ThermoFisher Scientific, USA) and a M5 Pic5 Green dsDNA Assay Kit (Mei5 Biotechnology, China), respectively.

Measurement of c-di-GMP level

Intracellular c-di-GMP concentrations in *V. parahaemolyticus* cells were measured similarly to those previously described (Zhang et al. 2023d). Briefly, the bacterial seed was diluted 1, 000-fold into 5 ml of LB-0.5% NaCl and then incubated at 37 °C with shaking at 200 rpm. Bacterial cells were harvested at the mid-log growth phase ($OD_{600} \approx 1.4$), washed twice with ice-cold PBS, and then resuspended in 1 ml of ice-cold PBS, followed by sonication for 5 min. After centrifugation, the intracellular c-di-GMP concentration and total proteins in the supernatant were measured using a c-di-GMP enzyme-linked immunosorbent assay (ELISA) kit (Mskbio, China) and a Pierce BCA Protein Assay kit, respectively. The intracellular c-di-GMP level was calculated as pmol/g of protein.

RNA isolation and quantitative real-time PCR (qPCR)

Bacterial cells of *V. parahaemolyticus* strains were harvested during the mid-log growth phase, at which the OD_{600} value was approximately 1.4. Subsequently, total RNA was extracted using TRIzol Reagent (Invitrogen, USA). cDNA was generated from 1 µg of total RNA using a FastKing First Strand cDNA Synthesis Kit (Tiangen Biotech, China). qPCR was performed on a LightCycler 480 (Roche, Switzerland) with a SYBR Green master mixture. Relative gene expression was determined using the $2^{-\Delta\Delta Ct}$ method, with 16 S rRNA serving as the internal control (Gao et al. 2011). All primers used in this study are listed in Table 1.

Statistical methods

The CV staining assay, colony morphology assay, motility assays and measurement of growth curves were performed at least twice, with the presentation of similar results. Measurement of c-di-GMP level, extracellular proteins, and eDNA, as well as qPCR, were performed at least three times. The results were expressed as the mean ± standard deviation (SD). Student's *t*-tests were used to calculate the statistical significance, with a p value less than 0.05 considered significant.

Table 1 Oligonucleotide primers used in this study

Target	Primers (forward/reverse, 5'-3')
Construction of mutants	
icmF2	GTGACTGCAGTATGGGTGGTTTGTTCGG/GCG GAGCTCTGATTCAATATGAGTAGAG
	CTTGGCACGGTTTCTTAGGG/ TCGTCAGCAGA ACATAGATTGG
	CGGGGTACCATGAGTATTAAAGAAATAGGCAG AG/GCGGTCGACTTACAAGGTTTGCGGACATC
Construction of complemented mutant	
icmF2	CGGGGTACCATGAGTATTAAAGAAATAGGCAG AG/GCGGTCGACTTACAAGGTTTGCGGACATC
qPCR	
cpsA	GAGAGCGGCAACCTATATCG/CGCCACGCCAA CAGTAATG
mfpA	GCGGGCAATGATCGTCTAAC/TCACCTGAACC TGCGACAAG
scrJ	GCTGTTAAAAGTCGCTGCTA/TGTTGTCGCTCT AAGTTCTCG
scrL	CCGTTCTATGGGTAAGCCTC/CTGGCATATCGT CAGGTAGG
vopY	TTTTCAGGATACGAGGTA/GAAGTGATGCGTG TTGTT
tpdA	AGAATCAACCAACACACGAA/CACAATACTGT TGATGGCGTA
gefA	GCTTTACAACAACTACGTGG/GGTATCTGACA AAGTATCAC
scrA	CACACCACGAACACATTGC/TCAATAGCGTCA CGGAATGC
scrG	AAGCCGTGGTGGAAGAAGG/GCGTGTTGAGT GCGTTGG
16 S rRNA	GACACGGTCCAGACTCCTAC/GGTGCTTCTTC TGTCGCTAAC

Results

IcmF2 promoted biofilm formation by*V. parahaemolyticus*in low salt conditions

Previously, our lab routinely used M broth to culture *V. parahaemolyticus* at 30ºC with shaking at 150 rpm to investigate its biofilm formation ability (Zhang et al. 2021, 2023d, f). In this study, the CV staining assay was employed to determine whether IcmF2 has a regulatory effect on the biofilm formation of *V. parahaemolyticus* under this growth condition. As shown in Fig. 1a, the Δ*icmF2* strain produced similar CV staining results to the WT strain under all the tested time points, suggesting that IcmF2 did not have a regulatory effect on the biofilm formation of *V. parahaemolyticus* in marine-like growth conditions. *V. parahaemolyticus* is also capable of forming biofilms in nutrient-rich media such as Heart Infusion broth (Li et al. 2021). Therefore, *V. parahaemolyticus* strains were grown in nutrient-rich LB broth containing different concentrations of NaCl to quantify biofilms and compare colony morphology variations. As shown in Fig. 1b, the Δ*icmF2* strain produced significantly less normalized CV staining compared to the WT strain under conditions of LB-0.5% NaCl and LB-1.0% NaCl ($P < 0.05$), while no significant differences in CV staining were observed between the Δ*icmF2* and WT strains under the growth condition of LB-1.0% NaCl ($P > 0.05$). As further determined by the colony morphology assays (Fig. 1c), the Δ*icmF2* strain exhibited less winkled colonies relative to the WT strain on LB plates containing 0.5% or 1.0% NaCl, while both the Δ*icmF2* and WT strains exhibited smooth phenotypes on plates containing 3.0% NaCl. In addition, the biofilm formation capacities of both Δ*icmF2* and WT under the growth condition of 0.5% NaCl were much stronger than those under the conditions of 1.0% and 3.0% NaCl (Fig. 1b and c). Moreover, there were no differences in growth rates between the Δ*icmF2* and WT strains under the conditions of LB-0.5% NaCl, LB-1.0% NaCl, and LB-3.0% NaCl, suggesting that the deletion of *icmF2* did not affect the growth of *V. parahaemolyticus* (Fig. 1d). In summary, these results suggested that IcmF2 promotes biofilm formation in *V. parahaemolyticus* under conditions with low salinities, and *V. parahaemolyticus* also exhibits a stronger biofilm formation capacity under the low salt condition.

IcmF2 did not regulate the swimming and swarming motility of

The diameters of swimming and swarming circles of the Δ*icmF2* and WT strains were measured and compared to assess whether IcmF2 affects the flagella-propelled motilities of *V. parahaemolyticus* in LB medium with varying concentrations of NaCl. As shown in Fig. 2, there were no significant differences in both swimming and swarming motility between Δ*icmF2* and WT under all tested growth conditions and all time points, suggesting that IcmF2 did not affect the swimming and swarming motility of *V. parahaemolyticus*. However, it appears that the higher the salinity of the medium, the stronger the motor capacity of *V. parahaemolyticus*, which might be due to the promotional effect of salinity on bacterial growth.

Incubation time affected IcmF2-dependent biofilm formation

V. parahaemolyticus had a stronger ability to form biofilms at a salinity of 0.5% NaCl than the other tested salinities, and thus the growth condition of 0.5% NaCl was chose to perform the following experiments. CV staining assays were performed to detect whether incubation time affects IcmF2-dependent biofilm formation. As shown in Fig. 3, the highest biofilms produced by Δ*icmF2* and WT were observed at an incubation time of 12 h, but a significant difference in biofilm formation capacity between the two strains were

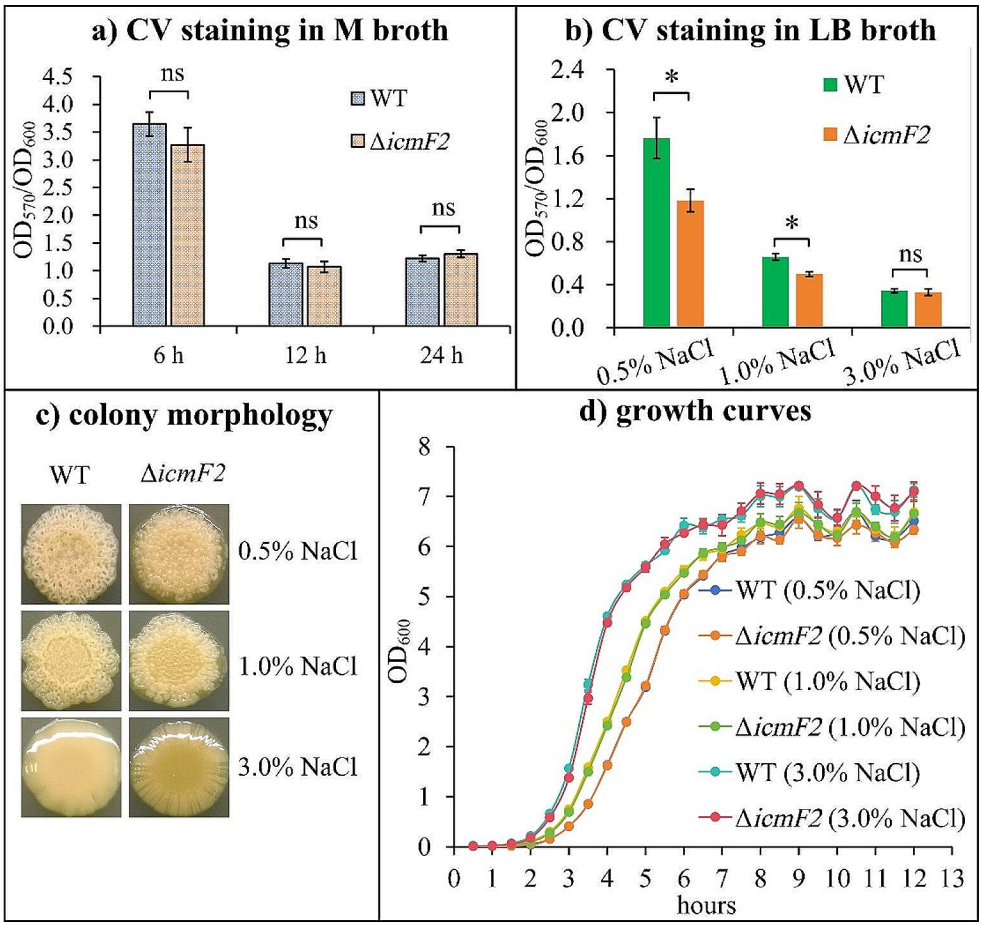

Fig. 1 Regulation of IcmF2 on biofilm formation by **V. parahaemolyticus**. The asterisks represent a *p* value less than 0.05, while 'ns' indicates a *p* value higher than 0.05. The biofilm formation capacities of the Δ*icmF2* and WT strains were assessed using crystal violet staining (**a** and **b**) and colony morphology (**c**). The images of the colony morphology assay are representative of at least three independent experiments. Growth curves of Δ*icmF2* and WT were created using a microbial growth curve analyzer MGC-200 by detecting OD_{600} values at a 30 min interval (**d**)

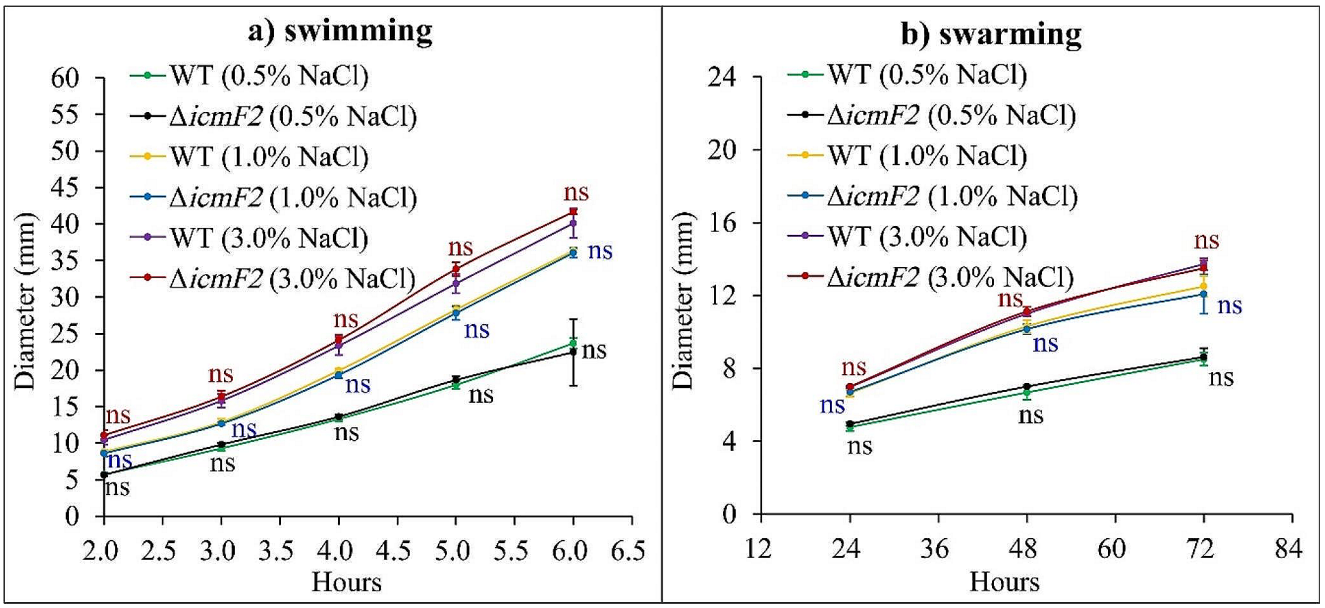

Fig. 2 Regulation of IcmF2 on swimming and swarming motility of *V. parahaemolyticus*. The swimming (**a**) and swarming (**b**) motility of Δ*icmF2* and WT were evaluated by detecting the diameters of swimming and swarming circles in HI plates containing different concentrations of NaCl, respectively. The results were presented as the mean ± standard deviation (SD). The 'ns' means a *p* value higher than 0.05

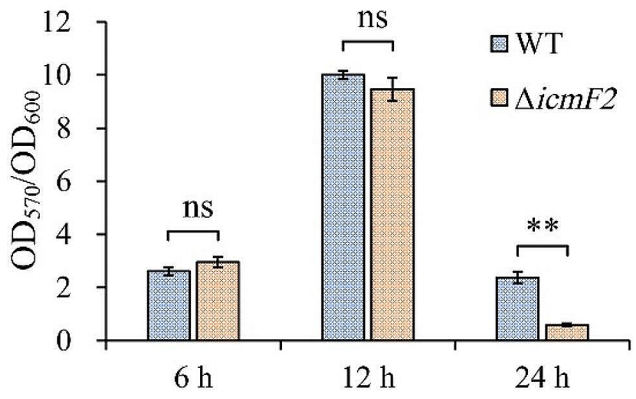

Fig. 3 Incubation time affected IcmF2-dependent biofilm formation. The CV staining assay was employed to detect whether incubation time affects IcmF2-dependent biofilm formation under the low salt growth condition. The double asterisks indicate statistically significant difference with a p value less than 0.01, whereas 'ns' indicates no statistically significant difference ($p > 0.05$)

only observed at an incubation time of 24 h ($P < 0.01$). Therefore, incubation time was able to influence the regulation of biofilm formation by IcmF2 in *V. parahaemolyticus*.

IcmF2 affected the contents of biofilm matrix components and c-di-GMP production

The main components of the biofilm matrix, which are essential for biofilm stability, include EPS, eDNA, extracellular proteins, and lipids (Flemming and Wingender 2010). The data presented here showed that the Δ*icmF2* strain produced significantly less eDNA and proteins in the biofilm matrix than the WT strain (Fig. 4a and b). In addition, the Δ*icmF2* strain also produced much less c-di-GMP than the WT strain (Fig. 4c). These results indicated that IcmF2 was capable of promoting the production of the main components of biofilm matrix and c-di-GMP in *V. parahaemolyticus*.

IcmF2 regulated the transcription of biofilm-associated genes

In this study, *cpsA*, the first gene of the *cpsA-K* operon responsible for EPS production (Liu et al. 2022), *mfpA*, which encodes the membrane fusion protein A contributing to biofilm formation (Enos-Berlage et al. 2005), and known c-di-GMP metabolism enzymic genes including *scrJ* (Kimbrough and McCarter 2021), *scrL* (Kimbrough and McCarter 2021), *vopY* (Wu et al. 2023), *tpdA* (Martínez-Méndez et al. 2021), *gefA* (Zhong et al. 2022), *scrABC* (Boles and McCarter 2002) and *scrG* (Kim and McCarter 2007), were selected as target genes for qPCR to investigate whether IcmF2 has regulatory effects on their transcription. As shown in Fig. 5, the mRNA levels of *cpsA*, *mfpA*, *scrJ*, *scrL*, *vopY*, *tpdA*, *gefA*, and *scrG* were significantly lower in the Δ*icmF2*/pBAD33 strain compared to the WT/pBAD33 and C-Δ*icmF2* strains. In contrast, the mRNA level of *scrA* was significantly higher in the Δ*icmF2*/pBAD33 strain. Furthermore, the expression of these genes was restored in the C-Δ*icmF2* strain when compared to the WT/pBAD33 strain. These results suggested that IcmF2 inhibits the transcription of *scrABC* but promotes the transcription of the other tested target genes.

Discussion

The function of T6SS requires at least 13 conserved proteins, including membrane-associated proteins such as TssL, TssM, and TssJ, and the components of bacteriophage-like tail such as Hcp, VgrG, and TssB (Silverman et al. 2012). TssL, TssM, and TssJ form channels across the cell envelope that bind to the peptidoglycan layer through TssL (Silverman et al. 2012). Hcp forms a bacteriophage tail-like tubular structure, while VgrG resembles the tail-spike-like proteins on the tip of the Hcp tube (Silverman

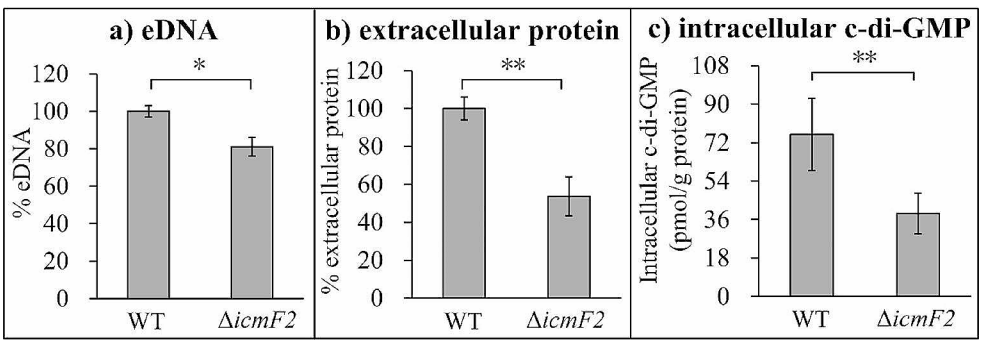

Fig. 4 Effect of IcmF2 on the production of eDNA, extracellular proteins and intracellular c-di-GMP.The effect of IcmF2 on the main components of biofilm matrix was assessed by detecting the relative contents of eDNA (**a**) and extracellular proteins (**b**). Intracellular c-di-GMP levels were measured using a c-di-GMP Enzyme-linked Immunosorbent Assay (ELISA) Kit (**c**). The double asterisks represent a p value less than 0.01, whereas the single asterisk indicates a p value less than 0.05

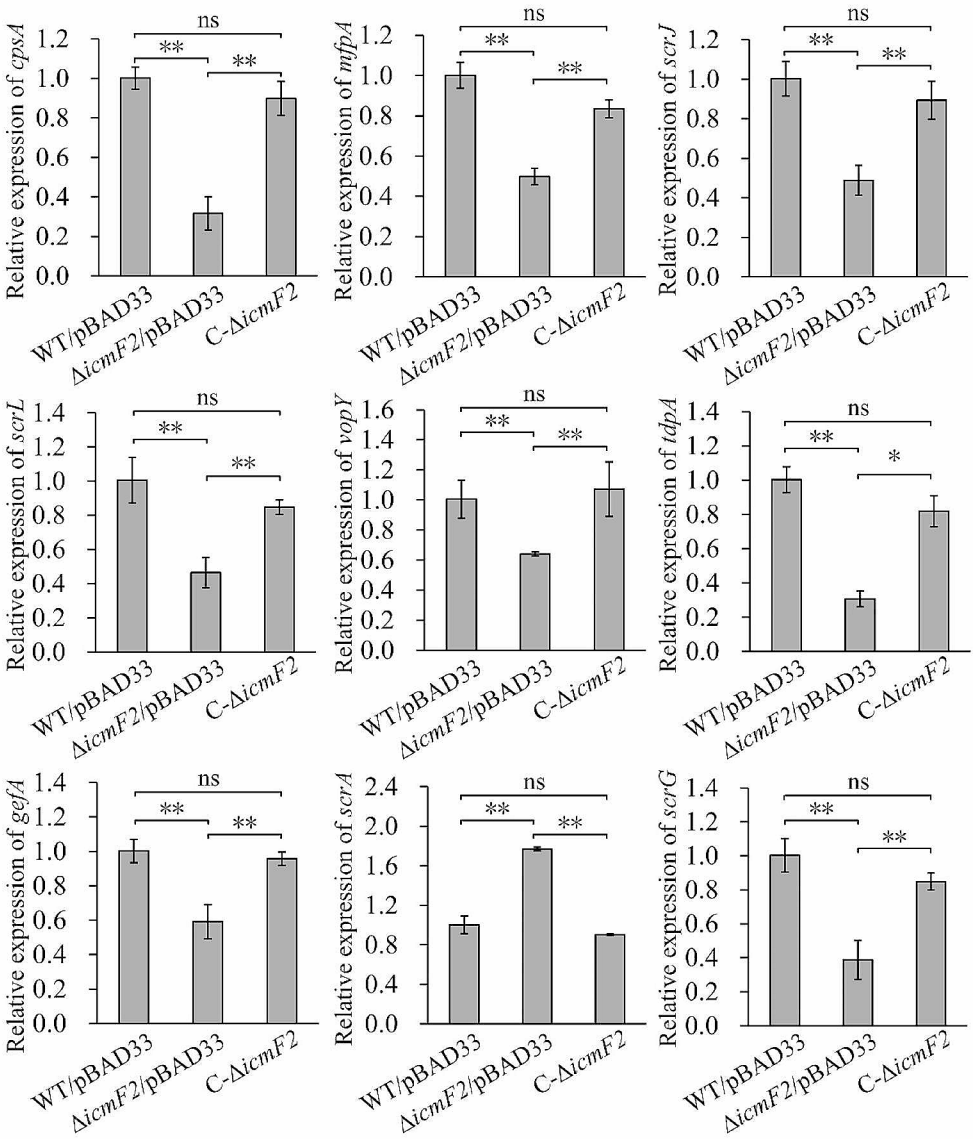

Fig. 5 Regulation of biofilm-related genes by IcmF2. Bacterial cells were harvested at an OD_{600} value of 1.4. The mRNA levels of each target gene were compared between WT/pBAD33, Δ*icmF2*/pBAD33, and C-Δ*icmF2*. The double (**) and single (*) asterisks denote a *p*-value less than 0.01 and 0.05, respectively, whereas the 'ns' indicates no statistically significant difference ($p > 0.05$)

et al. 2012). The Walker A motif of TssM is required for the secretion of Hcp and thus the function of T6SS (Ma et al. 2009; Silverman et al. 2012). In the T6SSs of some bacterial species, TssM is also named as IcmF, which is the homolog of TssM. Deletion of *icmF* from the genome of an avian pathogenic *E. coli* strain decreased adherence to and invasion of epithelial cells, intramacrophage survival, and biofilm formation capacity on abiotic surfaces (de Pace et al. 2011). In *V. cholerae*, deletion of *icmF* led to reduced motility but increased adherence to human intestinal epithelial cells and conjugation frequency (Das et al. 2002). *V. parahaemolyticus* possesses two kinds of T6SSs, namely T6SS1 and T6SS2, respectively (Makino et al. 2003). The *icmF1* or *hcp1* mutant of T6SS1 exhibited significantly reduced adhesion to Caco-2 and HeLa cells, whereas the *icmF2* or *hcp2* mutant of T6SS2 showed decreased adhesion only to HeLa cells (Yu et al. 2012). In addition, VgrG2 of *V. parahaemolyticus* T6SS2 was also able to induce autophagy in macrophages (Yu et al. 2015). However, the other roles that T6SS1 and T6SS2 may possess in *V. parahaemolyticus* remain obscure.

The data presented here demonstrated that IcmF2 promotes biofilm formation by *V. parahaemolyticus* in low salt conditions but does not in marine-like conditions (Fig. 1). However, the positive regulatory effect of IcmF2 on biofilm formation is limited, as the downregulation of the Δ*icmF2* strain results in less than a two-fold reduction in biofilm formation (Fig. 1b and c). Therefore, it is challenging for us to construct a complement strain through plasmid supplementation to verify the regulatory relationships. This is particularly true for the pBAD33 plasmid, which we frequently employed in previous studies (Sun et al. 2014; Chen et al. 2023; Zhang et al. 2023d, e). The use of this plasmid necessitates the addition of L-arabinose and chloramphenicol,

both of which significantly inhibit the biofilm formation of *V. parahaemolyticus* (Zhang et al. 2023a, b). Consequently, these additives would prevent us from observing the regulatory impact of IcmF2 on biofilm formation (data not shown). However, the data of qPCR assays confirmed that the *icmF2* mutation is non-polar (Fig. 4). Therefore, the conclusion that IcmF2 promotes biofilm formation is deemed reliable. Previously, T6SS2 has been demonstrated to be most active at cold and warm temperatures in low salt conditions, as the secretion of Hcp2 was only detected in low salt media at 23ºC and 30ºC (Salomon et al. 2013). It is logical that T6SS2 promotes biofilm formation only under low salt growth conditions. T6SS2 likely contributes, at least in part, to the robust biofilm formation capacity of *V. parahaemolyticus* under low salt growth conditions (Li et al. 2021). *V. parahaemolyticus* optimally grows at salinities ranging from 2 to 4%, but the human gut is a low salt environment relative to marine ecosystems (Whitaker et al. 2010). In addition, *V. cholerae* almost immediately forms biofilms after adhering to intestinal cells (Sengupta et al. 2016). T6SS2 also can be expressed at the temperature of 37ºC (Salomon et al. 2013). Further research is needed to determine whether *V. parahaemolyticus* can form biofilms in the intestine and whether T6SS2 plays a role in this process.

The data also showed that the influence of IcmF2 on biofilm formation was influenced by the incubation time, with significant differences in biofilm formation capacity between Δ*icmF2* and WT observed only at 24 h (Fig. 3). In addition, IcmF2 affected the production of eDNA, extracellular proteins and c-di-GMP (Fig. 5). eDNA and extracellular proteins, which are strongly positively correlated with the biofilm formation of *V. parahaemolyticus*, constitute the main components of the biofilm matrix (Flemming and Wingender 2010; Li et al. 2020). However, the specific role of IcmF2 in the secretion of extracellular DNA and proteins remains unclear. c-di-GMP is a second messenger that widely used by bacteria to control behaviors, including biofilm formation and motility (Homma and Kojima 2022). An elevated level of c-di-GMP in bacterial cells promotes biofilm formation but inhibits motility (Homma and Kojima 2022). Flagella-propelled swimming and swarming motility are required for the mature biofilm formation by *V. parahaemolyticus* (Yildiz and Visick 2009). However, the disruption of T6SS2 function did not affect the swimming and swarming motility of *V. parahaemolyticus* (Fig. 2), suggesting that T6SS2-dependent biofilm formation is not mediated by its influence on flagellar genes.

The *cpsA-K* and *scvA-O* operons are responsible for EPS production, but it is the *cpsA-K* operon that affects the colony morphology of *V. parahaemolyticus* on agar plates (Liu et al. 2022). Furthermore, the *mfpABC* operon, which encodes membrane fusion proteins, plays a positive role in biofilm formation by *V. parahaemolyticus* (Enos-Berlage et al. 2005). Deletion of *icmF2* resulted in a more than 2-fold downregulation of the transcription levels of *cpsA* and *mfpA* (Fig. 5), indicating that IcmF2 promotes biofilm formation partly by positively affecting the transcription of these two gene loci. The synthesis of c-di-GMP is catalyzed by the GGDEF domain of diguanylate cyclase (DGC), whereas the degradation of this molecule is catalyzed by the HD-GYP or EAL domain of phosphodiesterase (PDE) (Homma and Kojima 2022). In *V. parahaemolyticus*, ScrJ (Kimbrough and McCarter 2021), ScrL (Kimbrough and McCarter 2021), and GefA (Zhong et al. 2022) act as active DGCs, while VopY (Wu et al. 2023), TpdA (Martínez-Méndez et al. 2021), ScrC (encoded by *scrABC*) (Boles and McCarter 2002), and ScrG (Kim and McCarter 2007) are active PDEs. IcmF2 had positive effects on the transcription of *scrJ*, *scrL*, *vopY*, *tpdA*, *gefA*, and *scrG* (Fig. 5). Additionally, IcmF2 had a slight inhibitory effect on the transcription of *scrABC* (Fig. 5). Therefore, IcmF2-dependent c-di-GMP production in *V. parahaemolyticus* may be mediated by the influence of IcmF2 on the expression of these c-di-GMP metabolism-associated genes. However, *V. parahaemolyticus* harbors more than 60 putative enzymic genes that are likely involved in c-di-GMP metabolism (Römling et al. 2013). Thus, further studies should be conducted to elucidate the mechanisms of IcmF2 on c-di-GMP metabolism in *V. parahaemolyticus*.

In conclusion, this study reported that IcmF2 positively affects biofilm formation by *V. parahaemolyticus* under low salt conditions, and this effect is also influenced by the incubation time. IcmF2 was able to promote the production of eDNA, extracellular proteins, and c-di-GMP. In addition, the transcription of *cpsA*, *mfpA*, and a group of genes associated with c-di-GMP metabolism is shown to be influenced by IcmF2. Therefore, the promotion of biofilm formation by IcmF2 is likely mediated by its influence on the production of eDNA, extracellular proteins, and c-di-GMP, as well as the transcription of *cpsA*, *mfpA*, and a group of genes associated with c-di-GMP metabolism. This work confirms new physiological roles for IcmF2, which promotes biofilm formation and c-di-GMP production in *V. parahaemolyticus*.

Acknowledgements This work was supported by the Special Project on Clinical Medicine of Nantong University (2023JQ011 and 2023JQ017) and the Research Project of Nantong Health Commission (QN2023032).

Author contributions Q Huang, M Zhang, X Li and X Luo performed the laboratory experiments. S Ji, Y Zhang and R Lu designed and supervised the experiments. Q Huang and Y Zhang wrote the manuscript. Q Huang, M Zhang and X Li received the financial support. All authors read and approved the final manuscript.

Data availability All relevant data are within the manuscript.

Declarations

Competing interests The authors declare no competing interests.

References

Boles BR, McCarter LL (2002) Vibrio parahaemolyticus scrABC, a novel operon affecting swarming and capsular polysaccharide regulation. J Bacteriol 184:5946–5954. https://doi.org/10.1128/jb.184.21.5946-5954.2002

Chen L et al (2023) AphA directly activates the transcription of polysaccharide biosynthesis gene scvE in Vibrio parahaemolyticus. Gene 851:146980. https://doi.org/10.1016/j.gene.2022.146980

Coulthurst SJ (2013) The type VI secretion system - a widespread and versatile cell targeting system. Res Microbiol 164:640–654. https://doi.org/10.1016/j.resmic.2013.03.017

Das S, Chakrabortty A, Banerjee R, Chaudhuri K (2002) Involvement of in vivo induced icmF gene of Vibrio cholerae in motility, adherence to epithelial cells, and conjugation frequency. Biochem Biophys Res Commun 295:922–928. https://doi.org/10.1016/s0006-291x(02)00782-9

de Pace F et al (2011) Characterization of IcmF of the type VI secretion system in an avian pathogenic Escherichia coli (APEC) strain. Microbiol (Reading) 157:2954–2962. https://doi.org/10.1099/mic.0.050005-0

Enos-Berlage JL, Guvener ZT, Keenan CE, McCarter LL (2005) Genetic determinants of biofilm development of opaque and translucent Vibrio parahaemolyticus. Mol Microbiol 55:1160–1182. https://doi.org/10.1111/j.1365-2958.2004.04453.x

Flemming HC, Wingender J (2010) The biofilm matrix. Nat Rev Microbiol 8:623–633. https://doi.org/10.1038/nrmicro2415

Gallique M, Bouteiller M, Merieau A (2017a) The type VI Secretion System: a dynamic system for bacterial communication? Front Microbiol 8:1454. https://doi.org/10.3389/fmicb.2017.01454

Gallique M et al (2017b) Contribution of the Pseudomonas fluorescens MFE01 type VI Secretion System to Biofilm formation. PLoS ONE 12:e0170770. https://doi.org/10.1371/journal.pone.0170770

Gao H et al (2011) Regulatory effects of cAMP receptor protein (CRP) on porin genes and its own gene in Yersinia pestis. BMC Microbiol 11:40. https://doi.org/10.1186/1471-2180-11-40

Hespanhol JT, Nóbrega-Silva L, Bayer-Santos E (2023) Regulation of type VI secretion systems at the transcriptional, posttranscriptional and posttranslational level. Microbiol (Reading) 169. https://doi.org/10.1099/mic.0.001376

Homma M, Kojima S (2022) Roles of the second messenger c-di-GMP in bacteria: focusing on the topics of flagellar regulation and Vibrio Spp. Genes Cells 27:157–172. https://doi.org/10.1111/gtc.12921

Kim YK, McCarter LL (2007) ScrG, a GGDEF-EAL protein, participates in regulating swarming and sticking in Vibrio parahaemolyticus. J Bacteriol 189:4094–4107. https://doi.org/10.1128/jb.01510-06

Kimbrough JH, McCarter LL (2021) Identification of three New GGDEF and EAL Domain-containing proteins participating in the Scr Surface Colonization Regulatory Network in Vibrio parahaemolyticus. J Bacteriol 203. https://doi.org/10.1128/jb.00409-20

Li P et al (2017) Acute Hepatopancreatic Necrosis Disease-Causing Vibrio parahaemolyticus strains maintain an antibacterial type VI Secretion System with Versatile Effector repertoires. Appl Environ Microbiol 83. https://doi.org/10.1128/aem.00737-17

Li W et al (2020) Insights into the role of extracellular DNA and extracellular proteins in Biofilm formation of Vibrio parahaemolyticus. 11. https://doi.org/10.3389/fmicb.2020.00813

Li X et al (2021) The Effect of Salinity on Biofilm formation and c-di-GMP production in Vibrio parahaemolyticus. Curr Microbiol 79:25. https://doi.org/10.1007/s00284-021-02723-2

Li X et al (2024) Environmental magnesium ion affects global gene expression, motility, biofilm formation and virulence of Vibrio parahaemolyticus. Biofilm 7:100194. https://doi.org/10.1016/j.bioflm.2024.100194

Liu M, Nie H, Luo X, Yang S, Chen H, Cai P (2022) A polysaccharide biosynthesis locus in Vibrio parahaemolyticus important for Biofilm formation has Homologs widely distributed in aquatic Bacteria mainly from Gammaproteobacteria. mSystems 7:e0122621. https://doi.org/10.1128/msystems.01226-21

Lu R, Osei-Adjei G, Huang X, Zhang Y (2018) Role and regulation of the orphan AphA protein of quorum sensing in pathogenic Vibrios. Future Microbiol 13:383–391. https://doi.org/10.2217/fmb-2017-0165

Lu R et al (2019) Quorum sensing regulates the transcription of lateral flagellar genes in Vibrio parahaemolyticus. Future Microbiol 14:1043–1053. https://doi.org/10.2217/fmb-2019-0048

Ma LS, Lin JS, Lai EM (2009) An IcmF family protein, ImpLM, is an integral inner membrane protein interacting with ImpKL, and its walker a motif is required for type VI secretion system-mediated hcp secretion in Agrobacterium tumefaciens. J Bacteriol 191:4316–4329. https://doi.org/10.1128/jb.00029-09

Ma L et al (2012) Expression of the type VI secretion system 1 component Hcp1 is indirectly repressed by OpaR in Vibrio parahaemolyticus. ScientificWorldJournal 2012:982140. https://doi.org/10.1100/2012/982140

Makino K et al (2003) Genome sequence of Vibrio parahaemolyticus: a pathogenic mechanism distinct from that of V cholerae. Lancet 361:743–749. https://doi.org/10.1016/s0140-6736(03)12659-1

Martínez-Méndez R, Camacho-Hernández DA, Sulvarán-Guel E, Zamorano-Sánchez D (2021) A trigger phosphodiesterase modulates the global c-di-GMP Pool, Motility, and Biofilm formation in Vibrio parahaemolyticus. J Bacteriol 203:e0004621. https://doi.org/10.1128/jb.00046-21

Mougous JD et al (2006) A virulence locus of Pseudomonas aeruginosa encodes a protein secretion apparatus. Science 312:1526–1530. https://doi.org/10.1126/science.1128393

Park S, Sauer K (2022) Controlling Biofilm Development through cyclic di-GMP Signaling. Adv Exp Med Biol 1386:69–94. https://doi.org/10.1007/978-3-031-08491-1_3

Pukatzki S et al (2006) Identification of a conserved bacterial protein secretion system in Vibrio cholerae using the Dictyostelium host model system. Proc Natl Acad Sci U S A 103:1528–1533. https://doi.org/10.1073/pnas.0510322103

Römling U, Galperin MY, Gomelsky M (2013) Cyclic di-GMP: the first 25 years of a universal bacterial second messenger. Microbiol Mol Biol Rev 77:1–52. https://doi.org/10.1128/mmbr.00043-12

Salomon D, Gonzalez H, Updegraff BL, Orth K (2013) Vibrio parahaemolyticus type VI secretion system 1 is activated in marine conditions to target bacteria, and is differentially regulated from system 2. PLoS ONE 8:e61086. https://doi.org/10.1371/journal.pone.0061086

Sana TG et al (2016) Salmonella Typhimurium utilizes a T6SS-mediated antibacterial weapon to establish in the host gut. Proc Natl Acad Sci U S A 113:E5044–5051. https://doi.org/10.1073/pnas.1608858113

Sengupta C, Mukherjee O, Chowdhury R (2016) Adherence to Intestinal Cells Promotes Biofilm Formation in Vibrio cholerae. The Journal of Infectious Diseases 214:1571–1578 The Journal of Infectious Diseases

Sharan M, Vijay D, Dhaka P, Bedi JS, Gill JPS (2022) Biofilms as a microbial hazard in the food industry: a scoping review. J Appl Microbiol 133:2210–2234. https://doi.org/10.1111/jam.15766

Silverman JM, Brunet YR, Cascales E, Mougous JD (2012) Structure and regulation of the type VI secretion system. Annu Rev Microbiol 66:453–472. https://doi.org/10.1146/annurev-micro-121809-151619

Sun F et al (2014) H-NS is a repressor of major virulence gene loci in Vibrio parahaemolyticus. Front Microbiol 5:675. https://doi.org/10.3389/fmicb.2014.00675

Wang T et al (2015) Type VI Secretion System transports Zn2 + to Combat multiple stresses and host immunity. PLoS Pathog 11:e1005020. https://doi.org/10.1371/journal.ppat.1005020

Whitaker WB, Parent MA, Naughton LM, Richards GP, Blumerman SL, Boyd EF (2010) Modulation of responses of Vibrio parahaemolyticus O3:K6 to pH and temperature stresses by growth at different salt concentrations. Appl Environ Microbiol 76:4720–4729. https://doi.org/10.1128/aem.00474-10

Wu Q et al (2022) Transcriptomic Analysis of Vibrio parahaemolyticus underlying the wrinkly and smooth phenotypes. Microbiol Spectr 10:e0218822. https://doi.org/10.1128/spectrum.02188-22

Wu X et al (2023) Destruction of self-derived PAMP via T3SS2 effector VopY to subvert PAMP-triggered immunity mediates Vibrio parahaemolyticus pathogenicity. Cell Rep 42:113261. https://doi.org/10.1016/j.celrep.2023.113261

Yildiz FH, Visick KL (2009) Vibrio biofilms: so much the same yet so different. Trends Microbiol 17:109–118. https://doi.org/10.1016/j.tim.2008.12.004

Yu Y et al (2012) Putative type VI secretion systems of Vibrio parahaemolyticus contribute to adhesion to cultured cell monolayers. Arch Microbiol 194:827–835. https://doi.org/10.1007/s00203-012-0816-z

Yu Y, Fang L, Zhang Y, Sheng H, Fang W (2015) VgrG2 of type VI secretion system 2 of Vibrio parahaemolyticus induces autophagy in macrophages. Front Microbiol 6:168. https://doi.org/10.3389/fmicb.2015.00168

Zhang Y, Qiu Y, Tan Y, Guo Z, Yang R, Zhou D (2012) Transcriptional regulation of opaR, qrr2-4 and aphA by the master quorum-sensing regulator OpaR in Vibrio parahaemolyticus. PLoS ONE 7:e34622. https://doi.org/10.1371/journal.pone.0034622

Zhang Y et al (2017) Transcriptional regulation of the type VI Secretion System 1 genes by Quorum Sensing and ToxR in Vibrio parahaemolyticus. Front Microbiol 8:2005. https://doi.org/10.3389/fmicb.2017.02005

Zhang Y et al (2021) OpaR controls the metabolism of c-di-GMP in Vibrio parahaemolyticus. Front Microbiol 12:676436. https://doi.org/10.3389/fmicb.2021.676436

Zhang M et al (2023a) Effect of sublethal dose of chloramphenicol on biofilm formation and virulence in Vibrio parahaemolyticus. Front Microbiol 14:1275441. https://doi.org/10.3389/fmicb.2023.1275441

Zhang M et al (2023b) L-arabinose affects the growth, biofilm formation, motility, c-di-GMP metabolism, and global gene expression of Vibrio parahaemolyticus. J Bacteriol 205:e0010023. https://doi.org/10.1128/jb.00100-23

Zhang M et al (2023c) QsvR represses the transcription of polar flagellum genes in Vibrio parahaemolyticus. Microb Pathog 174:105947. https://doi.org/10.1016/j.micpath.2022.105947

Zhang M et al (2023d) QsvR and OpaR coordinately repress biofilm formation by Vibrio parahaemolyticus. Front Microbiol 14:1079653. https://doi.org/10.3389/fmicb.2023.1079653

Zhang Y et al (2023e) Quorum sensing and QsvR tightly control the transcription of vpa0607 encoding an active RNase II-type protein in Vibrio parahaemolyticus. Front Microbiol 14:1123524. https://doi.org/10.3389/fmicb.2023.1123524

Zhang Y et al (2023f) Transcriptomic profiles of Vibrio parahaemolyticus during Biofilm formation. Curr Microbiol 80:371. https://doi.org/10.1007/s00284-023-03425-7

Zhong X, Lu Z, Wang F, Yao N, Shi M, Yang M (2022) Characterization of GefA, a GGEEF domain-containing protein that modulates Vibrio parahaemolyticus Motility, Biofilm formation, and virulence. Appl Environ Microbiol 88:e0223921. https://doi.org/10.1128/aem.02239-21

Zhu W et al (2023) Identification of VP0143 gene which modulates biofilm formation of Vibrio parahaemolyticus. Food Bioscience 56:103271. https://doi.org/10.1016/j.fbio.2023.103271